

Supplementary Information

Development a Ratiometric Nitric Oxide Probe with Baseline Resolved Emissions by an ESIPT and Rhodol Ring Opened-closed Integrated Two-photon Platform

Xumei Wang ^a, Qi Sun ^a, Xinjian Song ^{a,*}, Yan Wang ^a, Wei Hu ^{b,*}

a. Hubei Key Laboratory of Biological Resources Protection and Utilization, School of Chemical and Environmental Engineering, Hubei University for Nationalities, Enshi, 445000, China. E-mail: whxjsong@163.com.

b. College of Bioresources and Materials Engineering, Shaanxi University of Science & Technology, Xi'an, 710021, China. E-mail: 4574@sust.edu.cn.

Table of Contents

1. Materials and instruments
2. Synthesis of Rh-NO-P
3. Fluorescent and absorption analysis
4. Supporting Table and Figures
5. References

1. Materials and instruments

Unless otherwise stated, all solvents and reagents were purchased from commercial suppliers and were used as received without further purification. BV-2 cells were obtained from Procell Life Science & Technology Co., Ltd. 3-(4,5-Dimethylthiazol-2-yl)-2,5-diphenyltetrazolium bromide (MTT), Lipopolysaccharide (LPS), NOC-9, amino-guanidine (AG), INF- γ , Apocynin and NS-398 were purchased from Sigma-Aldrich. All aqueous solutions were prepared in ultrapure water with a resistivity of 18.25 M Ω cm (purified by Milli-Q system, Millipore). High-resolution mass spectrometry was performed with LTQ FT Ultra (Thermo Fisher Scientific, America) in MALDI-DHB mode. NMR spectra were recorded on a Bruker-400 spectrometer, using TMS as an internal standard. The product of the currently used probe was detected by Agilent 1290 Infinity II/6230 TOF LC-MS system. Absorption spectra were recorded with a UV-vis spectrophotometer (Shimadzu UV-2550, Japan), and one-photon fluorescence spectra were obtained with a fluorimeter (Shimadzu RF-6000, Japan). Two-photon fluorescence spectra were excited by a mode-locked Ti:sapphire femto-second pulsed laser (Chameleon Ultra I, Coherent, America) and recorded with a DCS200PC photon counting with Omno- λ 5008 monochromator (Zolix, China). Two-photon microscopy (TPM) images were performed on a confocal laser scanning microscope (CLSM, C1-Si, Nikon, Japan).

2. Synthesis of Rh-NO-P.

The compound **Rh-NO-F** (100.00 mg, 0.19 mmol) and o-phenylenediamine (41.54 mg, 0.38 mmol) were dissolved in absolute ethanol (30.00 mL), and then added PyBop (10.00 mg, 0.02 mmol), and the solution was refluxed about 10 h by stirring. After the reaction, the solvent was distilled off under reduced pressure to obtain the crude product. Finally, the resulting solution was purified by silica column chromatography (petroleum ether/ethyl acetate = 2/1, v/v) to obtain a light yellow solid **Rh-NO-P**, the yield was 43%. ¹H NMR (600 MHz, DMSO-*d*₆) δ 8.10 – 7.92 (m, 4H), 7.80 – 7.65 (m, 4H), 7.48 – 7.26 (m, 4H), 6.87 (t, *J* = 7.7 Hz, 1H), 6.74 (s, 1H), 6.54 (d, *J* = 8.1 Hz, 1H), 6.23 (t, *J* = 7.6 Hz, 1H), 5.93 (d, *J* = 8.0 Hz, 1H), 4.42 (s, 2H), 3.33 (d, *J* = 7.4 Hz, 4H), 1.08 (t, *J* = 7.0 Hz, 6H). ¹³C NMR (150 MHz, DMSO-*d*₆) δ: 165.99, 157.66, 154.92, 152.97, 152.60, 151.66, 149.12, 146.27, 134.77, 133.90, 131.54, 129.57, 129.01, 128.39, 126.75, 125.26, 124.69, 123.57, 122.48, 122.30, 121.04, 116.60, 116.29, 109.12, 103.56, 97.66, 66.98, 44.14, 12.82. HR-MS (ESI) calcd for C₃₇H₃₀N₄NaO₃S⁺ [M+Na]⁺: 633.1936, found: 633.1900.

3. Fluorescent and absorption analysis.

Spectroscopic measurements. Unless otherwise mentioned, all the measurements for **Rh-NO-P** target reaction were tested in PBS buffer (10 mM, pH 7.4, containing 10% DMSO). After adding NO and incubating at 37°C for 5 min in a thermostat, a 500 μL aliquot of the reaction solution was transferred to a quartz cell with an optical length of 1 cm for the measurement of absorbance or fluorescence. The excitation wavelength was 800 nm, under two-photon excitation mode.

For the selectivity assay, superoxide anion ($\text{O}_2^{\cdot-}$) was prepared by dissolving KO_2 in DMSO solution. ^[1] $\cdot\text{OH}$ was generated by Fenton reaction between Fe^{2+} (EDTA) and H_2O_2 quantitatively, and Fe^{2+} (EDTA) concentrations represented $\cdot\text{OH}$ concentrations. ^[2] The ONOO^- source was the donor 3-morpholinopyridone hydrochloride (SIN-1, 100 μM). ^[3] NO was generated in form of 3-(aminopropyl)-1-hydroxy-3-isopropyl-2-oxo-1-triazene (NOC-5, 100 μM). ^[4] H_2O_2 was determined at 240 nm ($\epsilon_{240\text{ nm}} = 43.6\text{ M}^{-1}\text{cm}^{-1}$). NO_2^- was generated from NaNO_2 .

Determination of the detection limit. The limit of detection (LOD) for hypochlorous acid was calculated based on the following equation:

$$\text{LOD} = 3\sigma/k$$

Where σ represents the standard deviation and k represents the slope of the titration spectra curve among the limited range.

Quantum yield measurements. The measurement of the fluorescence quantum yield was measured by using an ethanol solution of rhodamine B as a standard (10 μM , $\Phi_r = 0.71$) and using the following equation.

$$\Phi_s = (A_r F_s n_s^2) / (A_s F_r n_r^2) \Phi_r \quad (A \leq 0.05)$$

Where s and r represent the sample to be tested and the reference dye, respectively. A represents the absorbance at the maximum absorption wavelength, F represents the fluorescence spectrum integral at the maximum absorption wavelength excitation, and n represents the refractive index of the sample to be tested or the reference dye solvent.

Measurement of Two-photon Cross Section. The two-photon absorption cross section (δ) was determined by using femtosecond (fs) fluorescence measurement technique as described. Rh-NO-P was dissolved in 10 mM PBS, and the two-photon induced fluorescence intensity was measured at 760-840 nm by using rhodamine B as the reference, whose two-photon property has been well characterized in the literature. The intensities of the two-photon induced fluorescence spectra of the reference and sample at the same excitation wavelength were determined. The TP absorption cross section was calculated by using the following equation.

$$\delta_s = (S_s \Phi_r n_s^2 c_r) / (S_r \Phi_s n_r^2 c_s) \delta_r$$

where the subscripts s and r stand for the sample and reference molecules, respectively. The intensity of the two-photon excited fluorescence was denoted as S. Φ is the fluorescence quantum yield, and Φ is the overall fluorescence collection efficiency of the experimental apparatus. The number density of the molecules in solution was denoted as c. δ_r is the two-photon absorption cross section of the reference molecule.

Cytotoxicity assay. The cytotoxicity was evaluated by MTT assay. Briefly, BV-2 cells were cultured in DMEM in 96-well microplates in incubator for 24 h. The medium was next replaced by fresh DMEM containing various concentrations of **Rh-NO-P** (0, 5, 10, 20, 30 μM). Each concentration was tested in five replicates. Cells were rinsed twice with phosphate buffer saline (PBS) 24 h later and incubated with 0.5 mg/mL MTT reagent for 4 h at 37 °C. The culture was removed and 150 μL DMSO was added to dissolve for mazan. After shaking for 10 min, the absorbance at 490 nm was measured by microplate reader (Synergy 2. BioTek Instruments Inc.). Cell survival rate was calculated by $A/A_0 \times 100\%$ (A and A_0 are the absorbance of the **Rh-NO-P** labelled group and the control group, respectively).

Cell culture and two-photon fluorescence imaging. BV-2 cells were cultured in DMEM supplemented with 1% penicillin/streptomycin and 10% fetal bovine serum (FBS), and incubated in an atmosphere of 5/95 (v/v) of CO_2/air at 37°C. For the four models that mimic the hypoxic ischemic process, the cells in group I were incubated with DMEM (no glucose) medium. BV-2 cells were plated into glass bottom cell culture dishes (NEST) in the day before imaging. Before the imaging experiments, the cells were washed with phosphate-buffered saline and then cultured with 5 μM **Rh-NO-P** (containing 1% DMSO in DMEM) for 30 min at 37°C. Two-photon microscopy (TPM) images were performed on a confocal laser scanning microscope (CLSM, C1-Si, Nikon, Japan). The TPM images were obtained from Channel 1 (blue, 410–530 nm) and Channel 2 (red, 580–650 nm) under excitation of 800 nm.

Calculation of mean fluorescence intensity. The mean fluorescence density was measured by Image-Pro Plus (v.

6.0) and calculated via the equation (mean density = $\text{IODsum}/\text{areasum}$), where IOD and area were integral optical density and area of the fluorescent region.

Immunofluorescence staining. wound healing-operated mice were euthanized and perfused with cold PBS, followed by fixation with 4% paraformaldehyde for 2 days. The ischemic brains were cut into 50- μm sections and the free-floating slices were blocked with 0.1 M PBS containing 5% fetal bovine serum and 0.3% Triton X for 1 h at room temperature. After washing, the slices were incubated at 4 °C overnight with the following primary antibodies: anti-IL-6 (1:200; 12912, Abcam, Cambridge, England). The slices were then rinsed anti- and incubated with an Alexa 594-conjugated antibody (1:200; ANT030, Millipore, Billerica, MA) or an Alexa 488-conjugated antibody (1:200; ANT024, Millipore, Billerica, MA) for 2 h at room temperature. All slices were photographed using a confocal fluorescence microscope (BX63, Olympus Optical Ltd, Tokyo, Japan). The number of immunoreactive cells in predefined areas were quantified using ImageJ software (Media Cybernetics Inc., Rockville, MD, USA). Six different fields for each mouse and six mice for each group were counted. All counts were conducted by blinded observers.

General procedure for detection of H_2O_2 , TNF- α and IL-1 β concentration. BV-2 cells were cultured in 96-well plates and treated with NS-398, APO after bearing LPS+INF/ γ . After treatment, cell culture supernatants were collected for detection of TNF- α concentration using TNF- α ELISA kit (Invitrogen, ERA56RB) and IL-1 β ELISA kit (Invitrogen, EHC002b) according to the manufacturer's instructions. Meanwhile, the cells were collected for measurement of cellular H_2O_2 concentration using the Amplex Red Hydrogen Peroxide Assay Kit (Invitrogen, A22188) according to recommended protocol as described earlier.

Histological Staining of the Tissue Slices. After imaging, the mice were killed, and the brains and other tissues (heart, liver, spleen, lung, kidney, stomach) were collected for tissue analysis. Through a series of standard procedures, including fixation in 10% neutral buffered formalin, embedding into paraffin and sectioning at 3 μm thickness, the tissues were stained with hematoxylin-eosin (H&E). Thereafter, the prepared slices were examined by a digital microscope.

Two-photon fluorescence imaging in tissue. All animal procedures were performed in accordance with the Guidelines for Care and Use of Laboratory Animals of South-central University of Nationalities and experiments were approved by the Animal Ethics Committee of College of Biology (South-central University of Nationalities). Wild-type C57BL/6J mice ($n = 300$; 25–30 g) were purchased from Hubei Experimental Animal Research Center. (Hubei, China; No. 43004700018817, 43004700020932). All animal experimental protocols were approved by the Animal Experimentation Ethics Committee of South-central University of Nationalities (No. 2020-scueec-043) and were conducted according to the Animal Care and Use Committee guidelines of South-central University of Nationalities. All BALB/c mice (age 4 weeks, weight 17–20 g) were randomly divided into Sham ($n = 3$), wound-control model ($n = 3$) and NS-398 model ($n = 3$) groups. Diabetic mice were prepared through intraperitoneal injection of streptozotocin (STZ, a diabetes-inducing drug), and man-made wounds were created on their right feet. 200 μL of 1.0 mM probe **Rh-NO-P** was intramuscularly injected to the wound margin and the mice were anesthetized, the wounded tissues were harvested and embedded in tissue-freezing medium, frozen and consecutively sectioned into slices. Then, the slices were washed with PBS three times and imaged by two-photon microscopy.

4. Supporting Table and Figures

Table S1. Photophysical properties of the dye **Rh-NO-F** in different solvents.

solution	$\lambda_{abs\ max}/nm^{[a]}$	$\epsilon/M^{-1}\cdot cm^{-1}[b]$	$\lambda_{em\ max}/nm^{[c]}$	$\Phi^{[d]}$
water	350 nm	31200	n.d. [e]	n.d.
CH ₃ CN	352 nm	37200	590 nm	n.d.
1,4-dioxane	349 nm	47000	591 nm	n.d.
DCM	350 nm	43200	588 nm	0.44
MeOH	351 nm	34100	584 nm	0.52
EtOH	359 nm	34100	583 nm	0.08
DMF	348 nm	33100	589 nm	0.53
DMSO	355 nm	52300	591 nm	0.61

[a] maximum absorption wavelength. [b] molar absorption coefficient. [c] maximum fluorescence emission wavelength.

[d] quantum yield. [e] n.d.: undetectable.

Table S2. Comparison of properties of **Rh-NO-P** probe and **Rh-NO-F** fluorescent group.

	MW	λ_{ex} (nm) [a]	ϵ (M ⁻¹ cm ⁻¹) [b]	λ_{em} (nm) [c]	Φ [d]	λ_{ex} (nm) [e]	$\delta\Phi$ (GM) [f]
Rh-NO-P	610.20	360	1.42*10 ⁵	457	0.41	800	49.5
Rh-NO-F	520.14	360	3.00*10 ⁵	611	0.56	800	189.8

[a] maximum absorption wavelength. [b] molar absorption coefficient. [c] maximum fluorescence emission wavelength. [d] quantum yield. [e] maximum two-photon excitation wavelength. [f] two-photon active cross section (1 GM = 1 × 10⁻⁵⁰ cm⁴ s photon⁻¹).

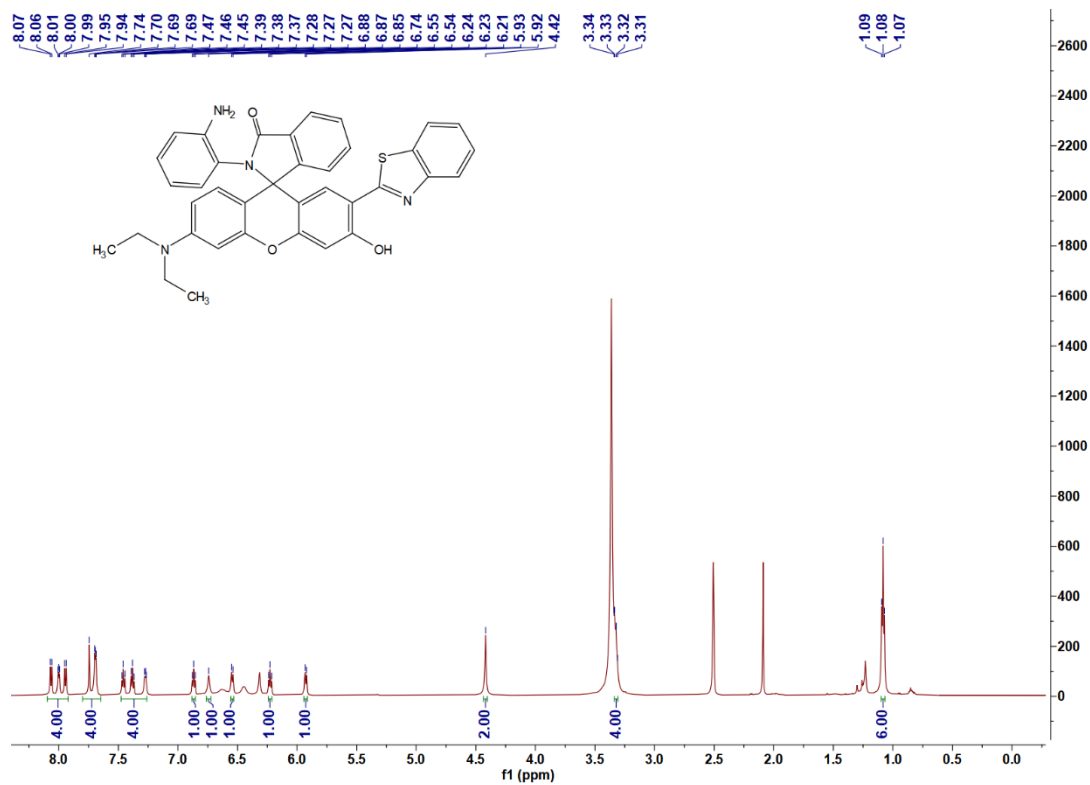


Fig. S1. ¹H NMR spectrum (600 MHz, DMSO-*d*₆) of probe Rh-NO-P.

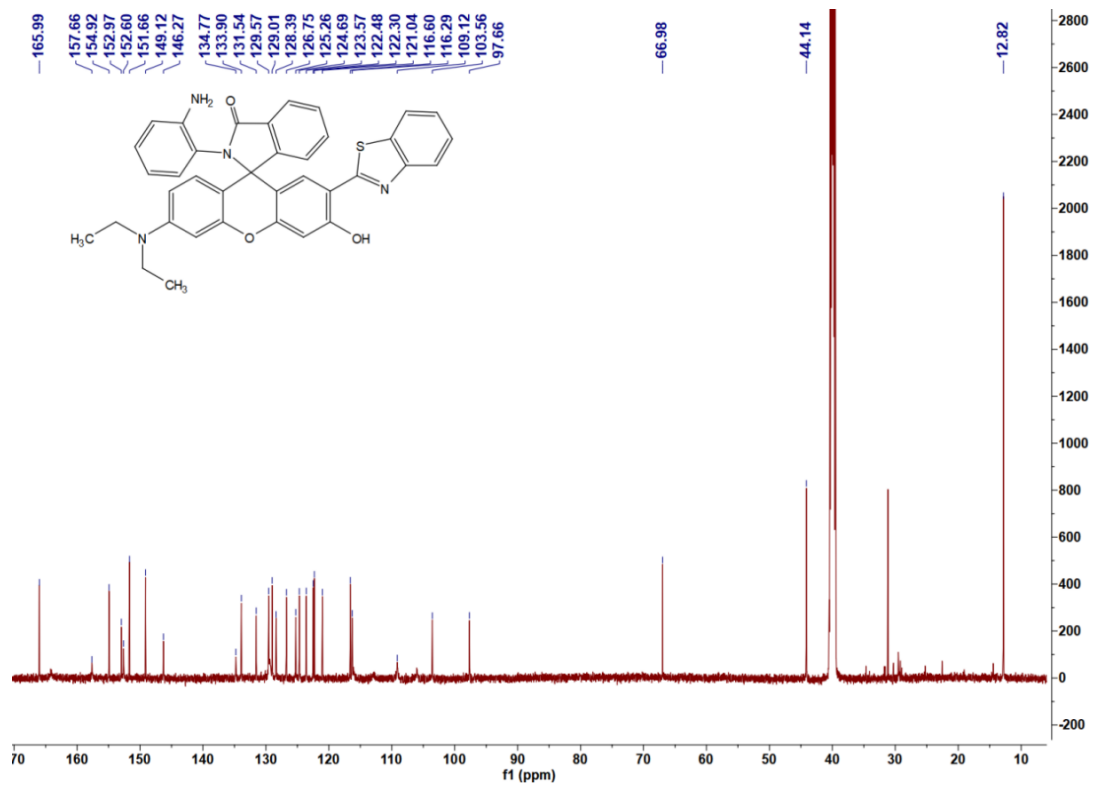


Fig. S2. ^{13}C NMR spectrum (150 MHz, $\text{DMSO-}d_6$) of probe **Rh-NO-P**.

Fig. S3. HR-MS spectrum of probe **Rh-NO-P**.

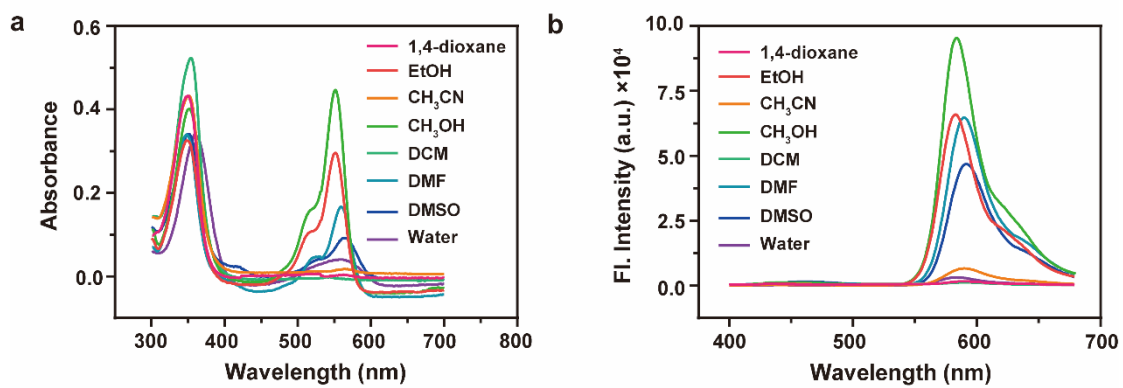


Fig. S4. Photophysical properties of fluorophore Rh-NO-F.

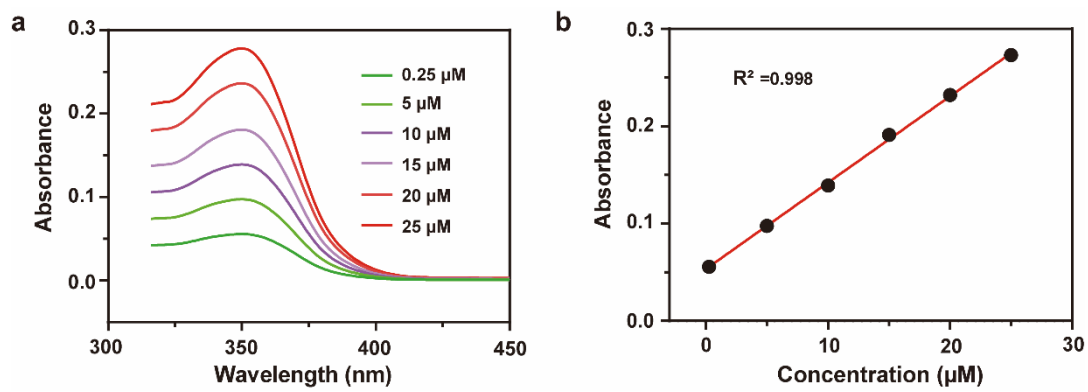


Fig. S5. Determination of solubility of probe Rh-NO-P.

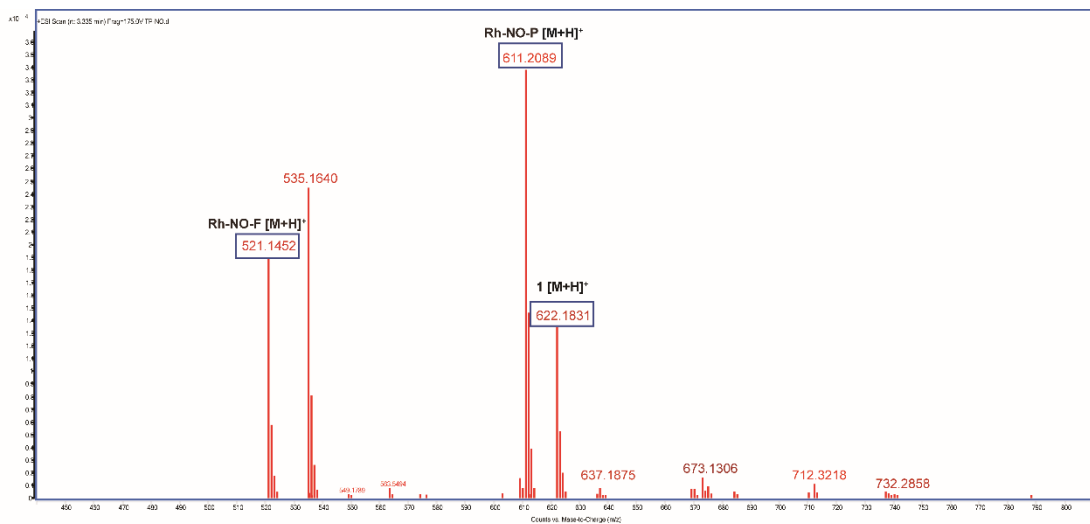


Fig. S6. HR-MS of probe **Rh-NO-P** after reaction with NO (1 eq) in PBS buffer solution for 20 s.

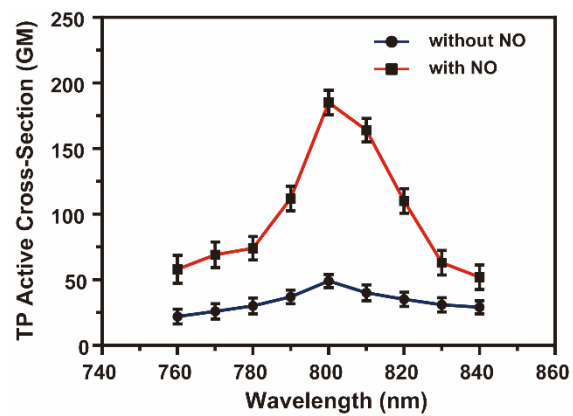


Fig. S7 Two-photon active absorption cross sections of **Rh-NO-P** probe (blue line) and **Rh-NO-F** (red line) at different wavelengths.

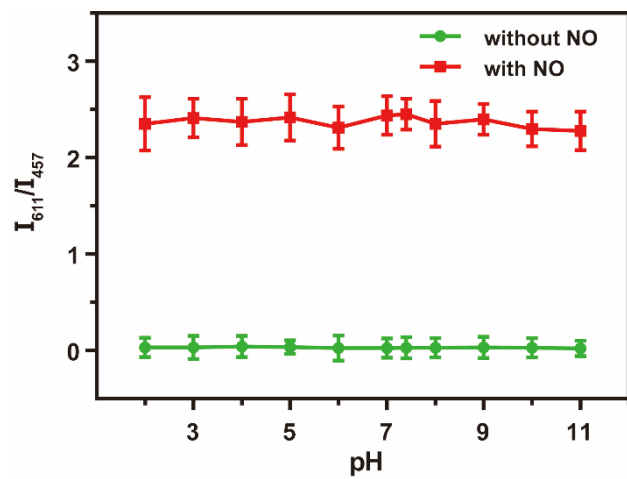


Fig. S8. The relationship between pH value and fluorescence intensity of **Rh-NO-P** before (green line) and after (red line) reaction with NO.

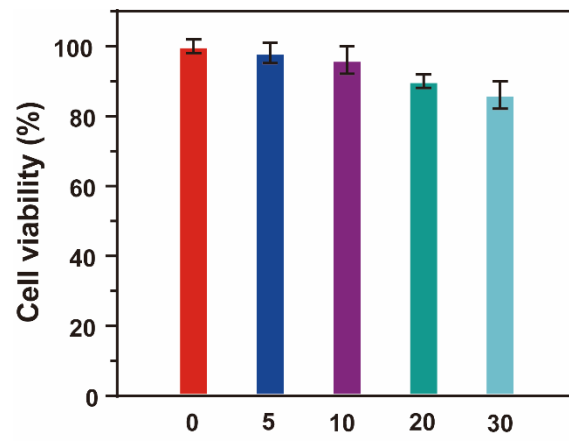


Fig. S9. MTT assay of BV-2 cells treated with different concentrations of **Rh-NO-P** (0, 5, 10, 20, 30 μM).

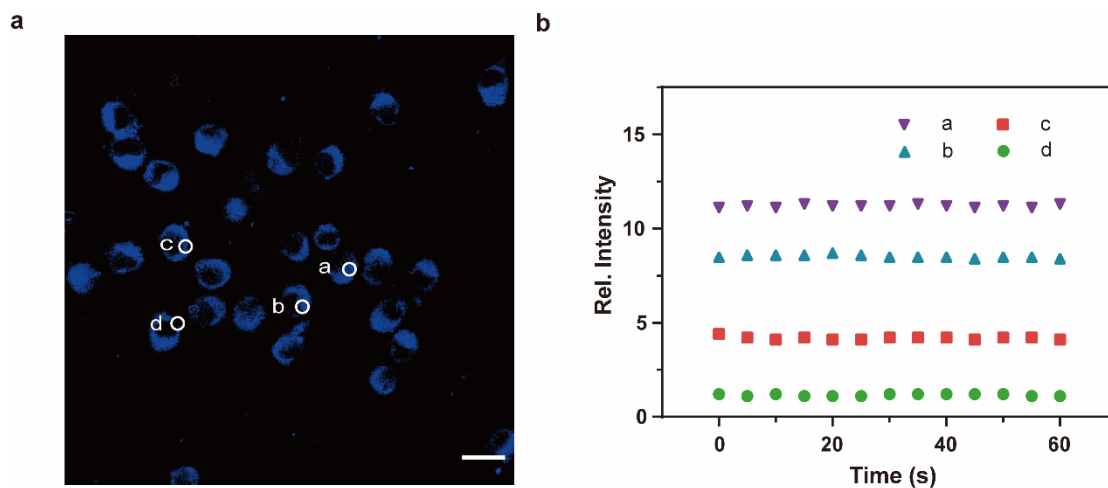


Fig. S10. a) TPM image of probe **Rh-NO-P** (10 μM); b) The relationship between the fluorescence intensity at points a, b, c and d versus time. Scale bar: 20 μm .

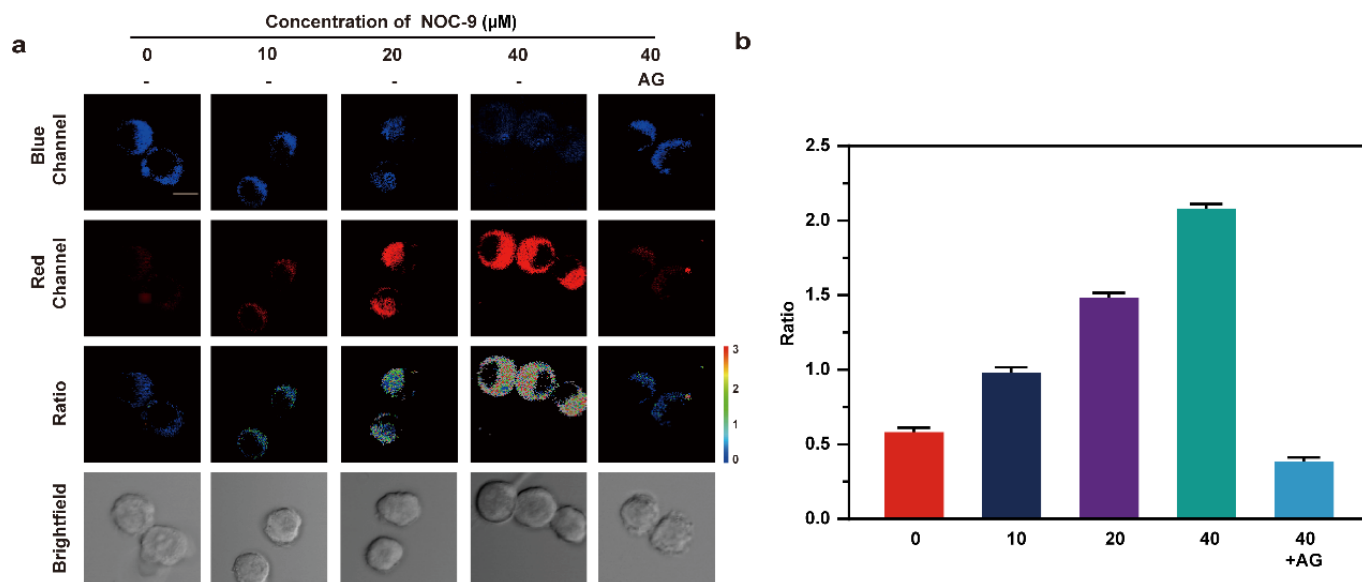


Fig. S11. (a) One-photon fluorescence images of BV-2 cells incubated with **Rh-NO-P**, obtained under different concentrations of NOC-9 (0, 10, 20, 40 μM) and 40 μM NOC-9 pretreated with AG (0.5 mM). (b) Mean intensity ratio of a). Emissions were collected at blue channel (420 ~ 530 nm) and red channel (580-650 nm) with 405 nm excitation. Scale bar: 50 μm . Data represent the mean of three replicates and the error bars indicate the SD (n = 21 cells from three independent cultures for each group).

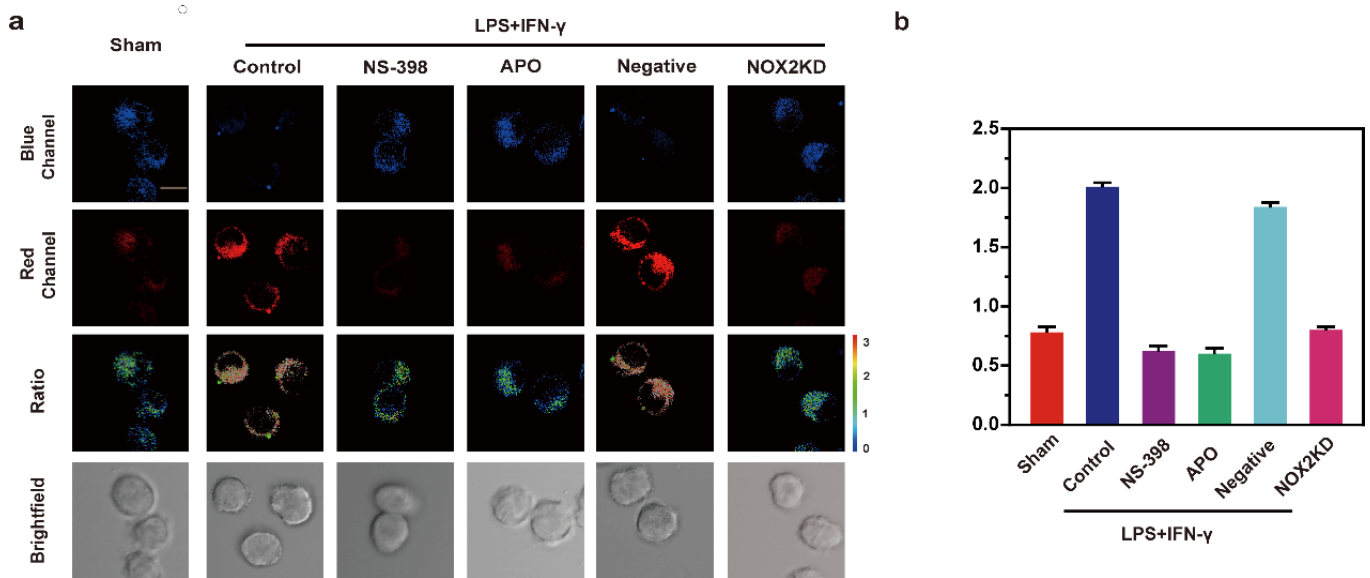


Fig. S12. (a) One-photon fluorescence imaging and (b) averaged fluorescence changes of **Rh-NO-P**-loaded (10 μ M) BV-2 cells when subjected to different treatments during LPS/IFN- γ induced inflammation: Sham group (untreated cells); control group (LPS/IFN- γ treated cells); NS-398 group (NS-398 treated cells during LPS/IFN- γ -induced inflammation); APO group (APO treated cells during LPS/IFN- γ -induced inflammation); negative group (negative control group of NOX2KD); and NOX2 KD group (NADPH oxidase 2 gene knockout). For the fluorescent images, the experiment was repeated using three cultures; similar results were obtained each time. Scale bar: 50 μ m. For changes in fluorescence: untreated cells, Sham group: n = 50 cells from three cultures; LPS/IFN- γ treated cells, control group: n = 59 cells from three cultures; NS-398 treated cells during LPS/IFN- γ -induced inflammation, NS-398 group: n = 48 cells from three cultures; APO treated cells during LPS/IFN- γ -induced inflammation, APO group: n = 62 cells from three cultures; negative control group of NOX2KD, negative group: n = 60 cells from three cultures; NADPH oxidase 2 gene knockout, NOX2KD group: n = 53 cells from three cultures.

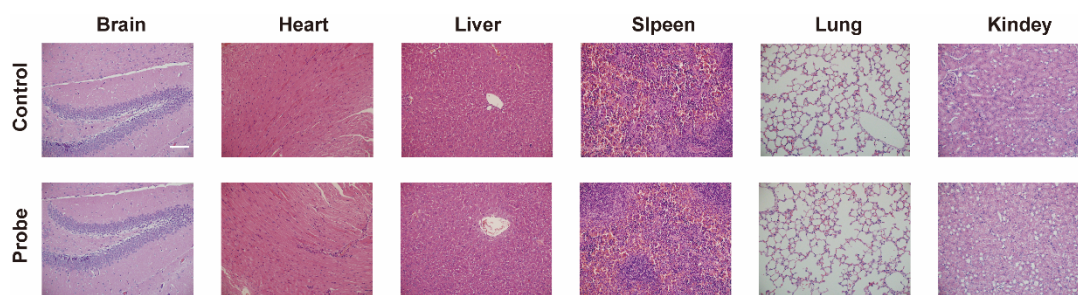


Fig. S13. H&E staining results of different organs collected from the control group and **Rh-NO-P** (200 μ L, 1 mM) treated group. Scale bar: 100 μ m.

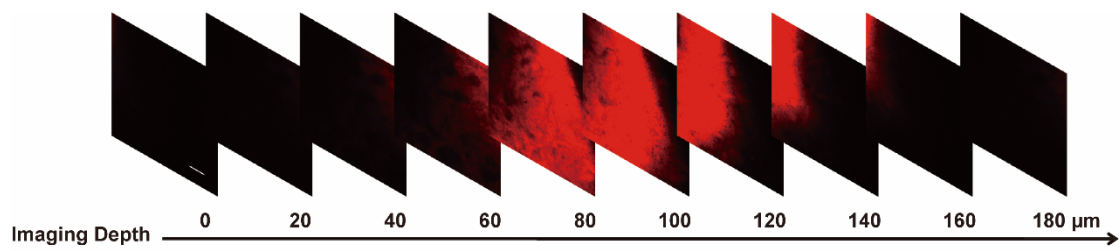


Fig. S14. Tissue imaging depth of probe **Rh-NO-P**. Scale bar: 50 μm .

References

- [1] M. Homma, Y. Takei, A. Murata, T. Inoue and S. Takeoka, *Chem. Commun.*, 2015, **51**, 6194–6197.
- [2] H. Zhang, W. Feng and G. Feng, *Dyes Pigment*, 2017, **139**, 73–78.
- [3] B. C. Dickinson, C. Huynh and C. J. Chang, *J. Am. Chem. Soc.*, 2010, **132**, 5906–5915.
- [4] M. Ren, B. Deng, K. Zhou, X. Kong, J. Y. Wang and G. Xu, *J. Mat. Chem. B*, 2016, **4**, 4739–4745.